optica

Light needles in scattering media using self-reconstructing beams and the STED principle: supplementary material

CRISTIAN GOHN-KREUZ AND ALEXANDER ROHRBACH*

Laboratory for Bio- and Nano-Photonics, Department of Microsystems Engineering---IMTEK, University of Freiburg, 79110 Freiburg, Germany
**Corresponding author: rohrbach@imtek.de*

Published 15 September 2017

This document provides supplementary information to "Light needles in scattering media using self-reconstructing beams and the STED principle," https://doi.org/10.1364/optica.4.001134.

https://doi.org/10.6084/m9.figshare.5315005

Gaussian background subtraction. Measuring the cross-section of a beam is often difficult. In case of free space propagation, a small mirror can be inserted in the beam path to deflect the beam directly to the camera. However, when the beam is propagating through a cluster of spheres (e.g., embedded in agarose gel) a mirror cannot be inserted, but the fluorescence excited by the beam can be imaged. This has the drawback that through the imaging process the 3D beam is convolved with the 3D detection point spread function of the microscope. The experimental data shown in Fig. 5 in the main article as well as in Fig. S1 below (black dotted line), reveal that the ring system of the Bessel beam is strongly suppressed by the imaging process. Since a 3D deconvolution is usually difficult and even impossible if no 3D data is available, an approximation is to subtract a Gaussian shaped background from the measured intensity profile, as illustrated by Fig. S1: The experimentally obtained profile from the image of a Bessel beam (black dotted line) resembles the sum of a Gaussian background function (blue solid line) and the profile from a simulated Bessel beam (red solid line).

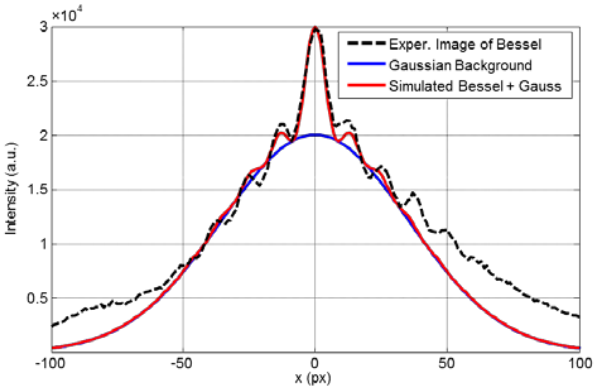

Fig. S1. Comparison between a measured intensity profile from an imaged Bessel beam and the sum of a Gaussian background with a simulated Bessel beam.

Deduction of the decay constants in strongly scattering media. As stated in Section 4.D "Beam penetration and fluorescence depletion in sphere clusters" of the main text, the beam propagation behavior was studied in three different bead clusters with volume concentrations c_1 = 0.13%, c_1 = 0.26% and c_3 = 0.52%. While the beam profiles for c_1 and c_3 are shown in Figs. 6(a)-6(d) of the main text, the beam profiles for c_2 are shown in Fig. S1.

In Figs. 6 and S1 a decay of the fluorescence signal with increasing volume concentration can be perceived. In order to minimize the influence of an inhomogeneous sampling due to the discrete nature of the microparticles the beam profiles were averaged over a range of as described in the main text. The penetration depth was determined for the central lobe of the Bessel beam, such that the following mean fluorescence signal is effectively analyzed:

$$\overline{F_{i,j}}(z) = \frac{1}{2r_0 \cdot \delta z}\int_{-r_0}^{r0} dx \int_{-\delta z/2}^{\delta z/2} dz'\, F_{i,j}(x, z+z').$$

Here r_0 is the 1st root of the Bessel beam, the index i describes the illumination modality (i=Bessel w/o STED, Bessel w/ STED, Gauss) and the index j describes the volume concentration (j=1: c_1=0.13%; j=2: c_2=0.26%, j=3: c_3=0.52).

An exponential decay is assumed for the z dependency of the mean fluorescence signal:

$$\overline{F_{i,j}}(z) = \overline{F_{i,0}}(z) \cdot \exp[-\mu_{i,j} \cdot z].$$

Here $\overline{F_{i,0}}(z)$ is the mean fluorescence signal of an ideal, unscattered illumination beam in illumination mode i and $\mu_{i,j}$ the corresponding decay constant in medium j.

Due to the fact that $\overline{F_{i,0}}(z)$ is not accessible we will further consider the relative fluorescence signal $\overline{F_{i,j}^{(rel)}}(z)$:

$$\overline{F_{i,j}^{(rel)}}(z) = \frac{\overline{F_{i,j}}}{\overline{F_{i,1}}} = \exp[-(\mu_{i,j} - \mu_{i,1}) \cdot z] = \exp[-\Delta\mu_{i,j} z].$$

By performing an exponential fit to $\overline{F_{i,j}^{(rel)}}(z)$ the relative decay constants $\Delta\mu_{i,j} = \mu_{i,j} - \mu_{i,1}$ can be extracted. It is straightforward to assume that the decay constants are proportional to the volume concentration such that $\mu_{i,j} \propto c_j$ as it is the case with Mie scattering for instance. Due to the fact that $c_3 = 2 \times c_2 = 4 \times c_1$ we can derive the following relationship for the decay constants:

$$\mu_{i,1} = \Delta\mu_{i,2} \qquad \mu_{i,2} = 2 \cdot \Delta\mu_{i,2} \qquad \mu_{i,3} = \Delta\mu_{i,3} + \Delta\mu_{i,2}.$$

Figure 6(i) shows the relative fluorescence signal $\overline{F_{i,j}^{(rel)}}(z)$ with the corresponding exponential fits. Figure 6(j) shows the decay constants derived from these fits. The penetration depths $d_{i,j} = 1/\mu_{i,j}$ are shown in Fig. S2(h).

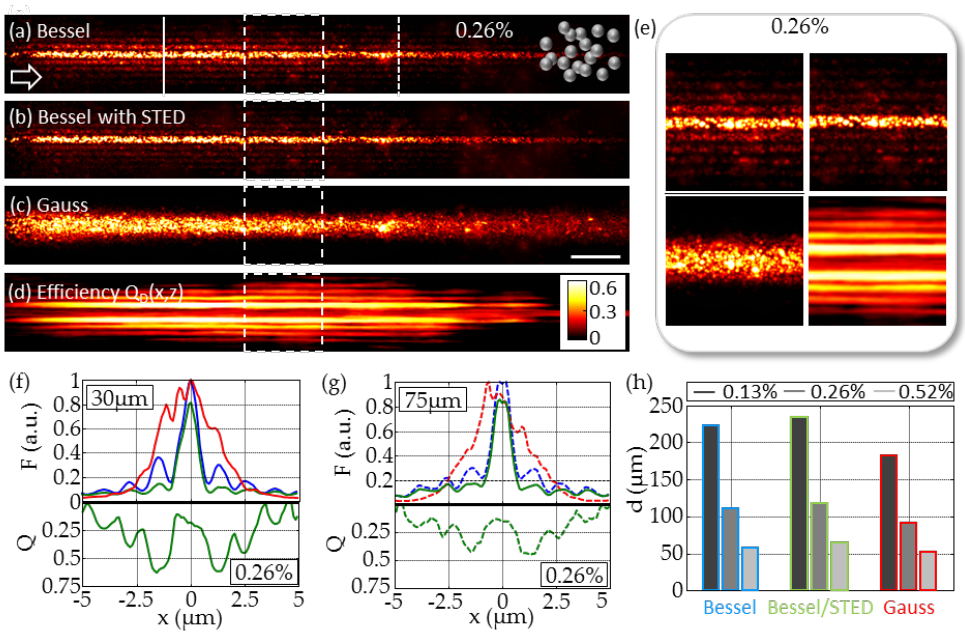

Fig. S2: Beam propagation over 120µm through a cluster of beads, fluorescence generation and STED efficiency. Fluorescencing polystyrene beads with 0.35 µm diameter are embedded in agarose gel at concentration c_2 = 0.26%. Maximum projections of images revealing (a) a single Bessel beam, (b) a Bessel beam with the STED beam, and (c) a Gaussian beam. (d) Space varying depletion efficiency Q_D (x,z) derived from (a) and (b). Central portions of (a)-(d) are magnified in (e). Fluorescence line profiles $F(x,z_0)$ at z_0 = 30µm (f) and z_0 = 75µm (g) and corresponding depletion efficiencies $Q_D(x,z_0)$. Profiles are averaged over 60 pixels, i.e., Δz≈6µm. (h) Penetration depths d derived from the decay constants shown in Fig. 6(j).